

Kuruppu, C, Pesiridis, A, Rajoo, S. (2014) Investigation of cylinder deactivation and variable valve actuation on gasoline engine performance. SAE Technical Papers, 1

This is a draft, pre-publication version of the paper.

# Investigation of Cylinder Deactivation and Variable Valve Actuation on Gasoline Engine Performance

**Author, co-author (Do NOT enter this information. It will be pulled from participant tab in MyTechZone)**

**Affiliation (Do NOT enter this information. It will be pulled from participant tab in MyTechZone)**

Copyright © 2014 SAE International

## Abstract

Increasingly stringent regulations on gasoline engine fuel consumption and exhaust emissions require additional technology integration such as Cylinder Deactivation (CDA) and Variable valve actuation (VVA) to improve part load engine efficiency. At part load, CDA is achieved by closing the inlet and exhaust valves and shutting off the fuel supply to a selected number of cylinders. Variable valve actuation (VVA) enables the cylinder gas exchange process to be optimised for different engine speeds by changing valve opening and closing times as well as maximum valve lift. The focus of this study was the investigation of effect of the integration of the above two technologies on the performance of a gasoline engine operating at part load conditions.

In this study, a 1.6 Litre in-line 4-cylinder gasoline engine is modelled on an engine simulation software and its data were analysed to show improvements in fuel consumption, CO<sub>2</sub> emissions, pumping losses and effects on CO and NO<sub>x</sub> emissions. A CDA and VVA operating window is identified which yields brake specific fuel consumption improvements of 10-20% against the base engine for speeds between 1000rpm to 3500rpm at approximately 12.5% load. Highest concentration of CO emissions was observed for BMEP in-between 4 bar to 5 bar at 4000rpm, and highest concentration of NO<sub>x</sub> found at the same load range but at 1000rpm. Findings based on simulation results point towards significant part load performance improvements which can be achieved by integrating cylinder deactivation and variable valve actuation on gasoline engines.

## Introduction

Despite the growing popularity and interest in Electric, Hybrid and other forms of alternative powertrains, the spark ignition (SI) gasoline engine still accounts for 44% of all new passenger car registration in Europe with diesel engines at 55% and all other technologies combined accounting for just 1% [1]. However, years of air pollution as a result of emissions from Internal Combustion (IC) engines and other power generation technologies has resulted in a plethora of technologies being pursued to offset the detrimental environmental impact.

Emissions from SI gasoline engines fall into two main categories; firstly, air pollutants which are Nitrogen Oxides (NO<sub>x</sub>), Carbon Monoxides (CO) and Hydrocarbons (HC), and secondly, the greenhouse gas (GHG) emissions such as Carbon Dioxide (CO<sub>2</sub>). The majority market share of IC engines is a main driving factor for increased emissions and fuel consumption, hence the stringent regulations imposed on new passenger cars.

To meet these regulations, current and future engines need to be designed and manufactured for increased engine efficiency and reduced fuel consumption which has proven to be directly related to reduce CO<sub>2</sub> emissions [2]. These targets can be met by employing a variety of technologies that are currently available and researched by scholars and engine manufacturers. However the commercial feasibility of the resulting technologies will be largely decided on their cost-to-benefit ratio, as the component incremental cost contributes towards the eventual and overall powertrain cost. The more immediate concern for improved engine efficiency and fuel economy is the consumers' desire to own and drive a more fuel efficient vehicle. This is not necessarily due to the environmental benefits of these technologies but the result of financial benefit of lower fuel consumptions; a survey indicated that 92% of owners consider fuel efficiency to be the most important purchasing criterion [3].

In most SI engines, engine load is controlled via a throttle valve which restricts the amount of air induced into the engine cylinders. By controlling the throttle valve, the amount of fuel injected is controlled in accordance to the desired air/fuel ratio. At Wide Open Throttle (WOT), the engine is operating at full load and in all other instances when the throttle valve is partially open, the engine is operating at some level of part load. An engine at part load has reduced indicated efficiency when compared to WOT due to the air flow restriction caused by the throttle valve which in turn increases the pumping losses. In typical driving conditions, engines operate mainly at part load conditions compared WOT. Therefore a standard SI engine is operating below its maximum potential during most of its operating life [4].

There are two valve technologies considered in this study. The first is the Variable valve actuation (VVA) technology which can be sub-categorised into Cam driven and Cam-less systems. In a standard cam driven valve train system, a camshaft with

specially shaped cam lobes is driven using the engine crankshaft at half the crankshaft speed. Cam-less systems use electro-magnetic, electro-hydraulic or electro-pneumatic systems to actuate each valve independently with complete control over the lift and/or timing as opposed to the limitation imposed by cam driven system due to the shape of the cam lobes profile. Therefore, cam-less systems offer a higher flexibility over cam driven systems, but are not without some drawbacks which are discussed in the subsequent section.

The principle behind Cylinder Deactivation (CDA) is the deactivation of cylinders in a multi-cylinder engine during part load operation to improve efficiency of the engine. This means that a higher displacement engine could be made to perform at the efficiency of a small displacement engine during CDA operation, which is why CDA engines are also referred to as variable displacement engines. By deactivating selected cylinders, the remaining working cylinders have to operate at a higher Indicated Mean Effective Pressure (IMEP) to maintain the same load, therefore the throttle valve is kept at a more open position than the case where all cylinders are activated, to allow more air into the working cylinders. Increased efficiency at part load operation with CDA has led to improved fuel consumption and reduced emissions [5].

However, NVH (Noise Vibration and Harshness) and driver requirements restrict the operating window of CDA [6]. Low frequency, high amplitude torque pulsations caused during CDA mode, as seen in Figure 1, is a key limiting factor when considering CDA operation for automotive applications. Active engine mounts and other NVH solutions have been investigated and integrated by automotive manufactures to overcome some of these issues [7].

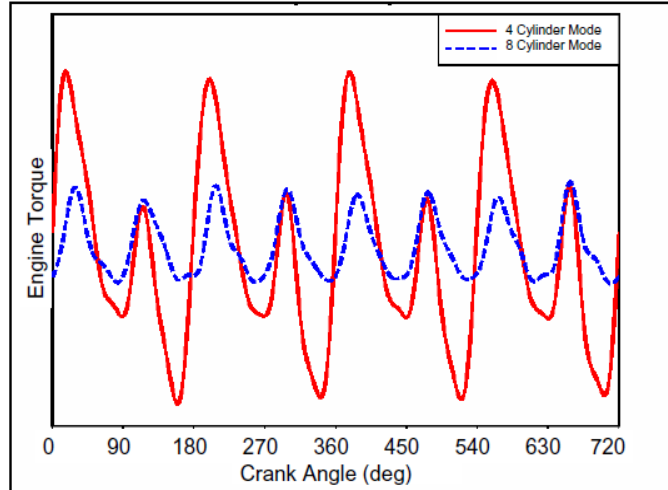


Figure 1 Engine torque pulsations [8]

## Methodology

In order to study the effects of VVA and CDA integration into a known engine, *Ricardo WAVE* 1D engine simulation software was used to model and simulate a 1.6L in-line, 4 cylinder, 16 valve gasoline engine. The experimental engine data used for the modelling were obtained from actual engine tests by [9] (and will be referred to as UTM data). The flowchart depicted in Figure 2 is an overview of the methodology used in this study.

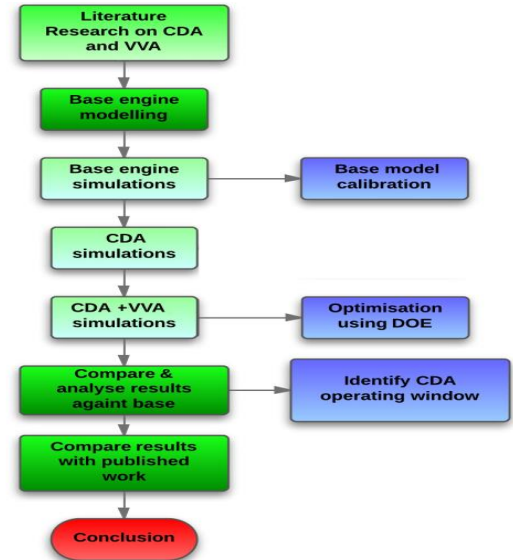


Figure 2 Methodology flowchart

### Base model simulation setup

Once the base model was tested for convergence and calibrated, simulations were carried out to gather data which was to be used later for comparisons against CDA and VVA simulations. The simulation matrix included 13 cases with engine speeds being varied from 1000 rpm to 7000 rpm in 500 rpm increments. The engine load was changed using the throttle valve angle which was varied in increments up to WOT using sub-cases within the 13 main cases. Therefore, each engine speed case had sub-cases where varying degrees of throttle angle were used to simulate engine load variations. The two main operating condition variables used in the simulations were engine speed and throttle angle. All simulations were carried out in steady state conditions.

### CDA+VVA model simulation setup

Following base engine simulations and data acquisition, the base engine valve models were modified to enable user defined maximum valve lift, maximum lift point and open duration for Intake and Exhaust Valves (IV and EV, respectively). The valve model also enabled valve deactivation by setting maximum valve lift to be zero. In order to simulate cylinder deactivation in the model, cylinders 2 and 3 which are alternative cylinders in the firing order were chosen to be deactivated. Similar CDA methods based on deactivating even number of cylinders in the firing order have been discussed by [5] and [8]. CDA was achieved by using the valve deactivation

method explained previously along with disabled fuel supply for the selected cylinders.

Following these modifications, the model is flexible enough to allow DOE techniques to optimise VVA strategy. Using the in-built DOE functionality of WAVE, a 2-level half factorial experiment consisting of 32 individual experimental points was carried out. EVDUR (EV open duration), EVML (EV max. lift), EVMP (EV max. lift point), IVDUR (IV Duration), IVML (IV max lift) and IVMP (IV max. lift point), were set as the parameter variables to maximise Brake Mean Effective Pressure (BMEP) and to minimise Brake Specific Fuel Consumption (BSFC) output which were the two of main targets considered in this study. The optimised valve parameters for inlet and exhaust are presented in Table 1 and Table 2.

Table 1 VVA inlet valve configuration

|             |     | Inlet                    |           |      |      |           | Standard valve |
|-------------|-----|--------------------------|-----------|------|------|-----------|----------------|
|             |     | VVA Valve configurations |           |      |      |           |                |
| Setting     | #   | 1                        | 2         | 3    | 4    | 5         |                |
| Speed range | rpm | 1000-2500                | 3000-5000 | 5500 | 6000 | 6500-7000 | All speeds     |
| Durraion    | deg | 254                      | 254       | 274  | 274  | 254       | 264            |
| Max Lift    | mm  | 4.05                     | 9.05      | 9.05 | 9.05 | 9.05      | 9.05           |
| Max Point   | deg | 458                      | 458       | 458  | 478  | 478       | 468            |

Table 2 VVA exhaust valve configuration

|             |     | Exhaust                  |           |           |           | Standard valve |
|-------------|-----|--------------------------|-----------|-----------|-----------|----------------|
|             |     | VVA Valve configurations |           |           |           |                |
| Setting     | #   | 1                        | 2         | 3         | 4         |                |
| Speed range | rpm | 1000-2000                | 3000-3500 | 4000-5000 | 5500-7000 | All speeds     |
| Durraion    | deg | 245                      | 255       | 245       | 255       | 255            |
| Max Lift    | mm  | 4.7                      | 8.7       | 8.7       | 8.7       | 8.7            |
| Max Point   | deg | 252.5                    | 252.5     | 252.5     | 252.5     | 252            |

## Analysis of data

Once the optimisation of the CDA+VVA model was completed, attention was focused on identifying the CDA operating window by using BMEP as the comparison factor. Simulations were carried out on both the base engine model and the CDA+VVA model with smaller throttle angle increments for the engine speed range between 1000rpm and 4000rpm. Similar engine speed ranges for CDA applications have been investigated by [5] and [10].

The BMEP results obtained from these tests were compared at the same engine speeds to identify similar load conditions and the throttle angle values which represented them were recorded. Performance data such as BSFC, brake power, brake torque, brake specific CO and NO<sub>2</sub> and Pump Mean Effective Pressure (PMEP) were then compared at the identified operating condition to analyse the effects of CDA+VVA integration.

## Results

Simulations were first carried out in base mode and followed by the CDA-only mode and finally the CDA+VVA model. The results for the Base model WOT simulations for a full engine speed sweep from 1000rpm to 7000 rpm are given in Table 3.

Table 3 Base model WOT performance

| Engine Speed                             | rpm      | 7000   | 6000   | 5000   | 4000   | 3000   | 2000   | 1000   |
|--|----------|--------|--------|--------|--------|--------|--------|--------|
| BMEP                                     | bar      | 10.36  | 11.15  | 12.43  | 12.10  | 11.00  | 10.97  | 9.48   |
| Brake Power                              | kW       | 96.53  | 89.01  | 82.73  | 64.41  | 43.92  | 29.19  | 12.62  |
| BSFC                                     | kg/kW/hr | 0.25   | 0.24   | 0.23   | 0.23   | 0.23   | 0.22   | 0.24   |
| PMEP                                     | bar      | -0.71  | -0.57  | -0.59  | -0.27  | -0.13  | -0.01  | -0.02  |
| Brake Torque                             | N*m      | 131.68 | 141.67 | 158.00 | 153.77 | 139.80 | 139.37 | 120.46 |
| Brake specific CO emissions              | g/kW/hr  | 12.07  | 10.68  | 11.75  | 15.07  | 15.48  | 15.84  | 15.34  |
| Brake specific NO <sub>2</sub> emissions | g/kW/hr  | 22.71  | 25.55  | 24.01  | 22.87  | 23.25  | 24.51  | 25.53  |
| Total volumetric efficiency              | -        | 0.89   | 0.91   | 1.01   | 0.95   | 0.86   | 0.85   | 0.78   |

## Model calibration

Calibrations were performed to gain an acceptable curve fit between the base simulation results and test engine (UTM data). The calibrated torque and power curves are given in Figure 3.

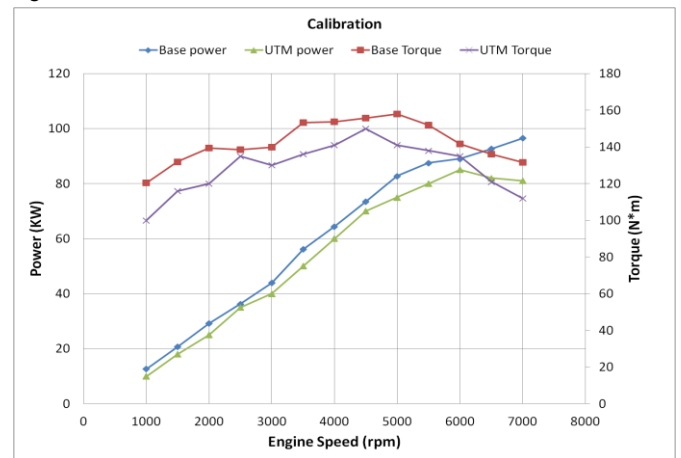


Figure 4 Base model WOT maximum cylinder pressure calibration curve fit

Further calibrations were performed using experimental maximum in-cylinder pressure data and simulated results. According to Figure 4 which shows the comparison of the maximum in-cylinder pressure data it is evident that the simulated results are within acceptable limits.

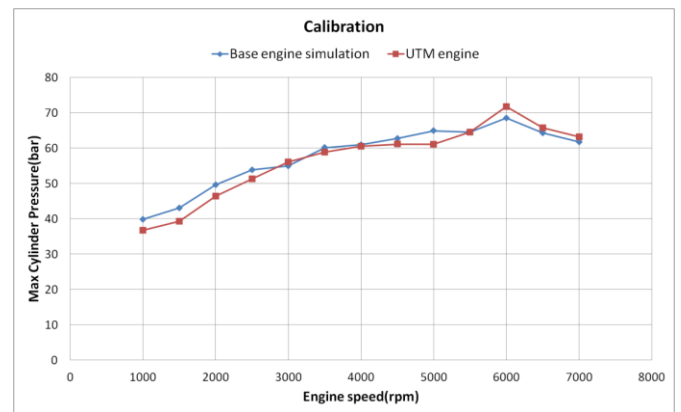


Figure 3 Base WOT power & torque calibration curve fit

## CDA+VVA WOT simulation results

The engine performance results of the CDA+VVA integrated model are presented in this section with comparisons against the CDA-only simulation results. A comparison as carried out to identify the contribution of each of the technologies (CDA and VVA) towards the overall performance benefits of the engine and is given in Figure 5. The results presented here are for a CDA+VVA model with optimised valve parameters.

BSFC, brake torque, brake power and total volumetric efficiency all show improvements up to 5000rpm while higher engine speeds do not show any significant improvements. This is partly due to limited power and torque availability in CDA+VVA operation at high engine speeds and also due to the increasing engine efficiencies of the base model engine with increasing speed as the throttle is opened. The performance benefits seen at 7000rpm are not consistent with this trend and therefore may be the result of the increased divergence of the calibrated engine model to the actual engine data at 7000 rpm.

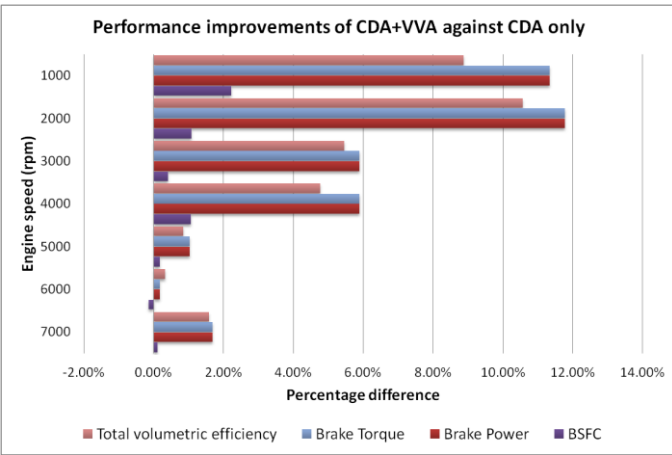


Figure 5 CDA+VVA WOT performance difference against CDA only

## Part load base simulation results

Thus far, all simulations have been for WOT (90 degrees throttle angle) conditions (full load). Therefore in this section, results are presented for simulated part load operation of the base engine. The throttle angle was used as the variable to control the load condition and throttle angles between 20-90 degrees (deg) were considered as part load.

Table 4 contains the simulated engine performance results at 30 deg throttle angle for seven engine speed cases. Throttle sweep simulations were carried out at 10 deg increments starting with 20 deg throttle angle and up to WOT. Individual throttle angle results are not presented here as they follow a similar pattern.

Table 1 Part load base simulation results (30deg throttle)

| Throttle Angle               | deg      | 30    |       |       |       |       |       |       |
|------------------------------|----------|-------|-------|-------|-------|-------|-------|-------|
| Engine speed                 | rpm      | 4000  | 3500  | 3000  | 2500  | 2000  | 1500  | 1000  |
| BMEP                         | bar      | 0.52  | 0.98  | 1.63  | 2.42  | 3.44  | 4.99  | 6.80  |
| Brake Power                  | kW       | 2.78  | 4.59  | 6.49  | 8.06  | 9.16  | 9.96  | 9.04  |
| BSFC                         | kg/kW/hr | 0.98  | 0.59  | 0.42  | 0.34  | 0.30  | 0.27  | 0.25  |
| PMEP                         | bar      | -0.83 | -0.78 | -0.69 | -0.60 | -0.52 | -0.41 | -0.22 |
| Brake Torque                 | N*m      | 6.63  | 12.51 | 20.66 | 30.80 | 43.76 | 63.40 | 86.35 |
| Brake specific CO emissions  | g/kW/hr  | 66.72 | 38.74 | 25.09 | 19.75 | 19.99 | 19.94 | 15.02 |
| Brake specific NO2 emissions | g/kW/hr  | 47.73 | 32.69 | 25.59 | 24.88 | 23.49 | 24.29 | 25.48 |
| Total volumetric efficiency  | -        | 0.18  | 0.20  | 0.24  | 0.28  | 0.35  | 0.47  | 0.60  |

Figure 6 shows the variation in cylinder pressure change against clearance volume for 30 deg throttle angle when compared against WOT. The pumping loss is represented by the lower portion of the plot for the 30 deg curve where it dips below the WOT curve. The pressure loss seen here is mainly due to the air restriction caused by the partially open throttle valve. The reduction in pressure for 30 deg throttle angle

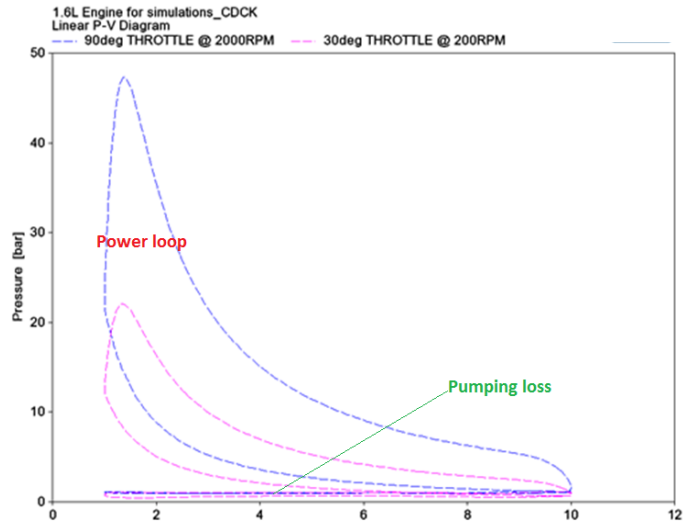


Figure 6 Part load base P-V diagram

against WOT (90 deg) seen in the upper portion of the curve, known as the power loop, is due to less fuel been injected into the engine in order to maintain constant air to fuel ratio resulting in reduced power.



The BSFC contour plots presented in Figure 7 are part load simulated results plotted against throttle angle and engine speed. Figure 7 shows that at smaller throttle angles, BSFC is higher and keeps increasing as the engine speed is increased.

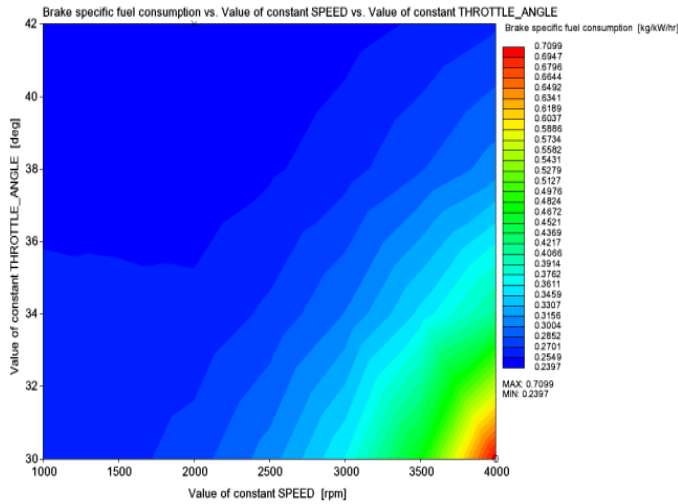


Figure 7 Part load base BSFC vs Throttle angle

The simulated CO emissions results of the base engine at part load are given in Figure 9. The test was conducted at throttle angles between 30-90 deg with engine speed being varied between 1000 - 4000rpm. The peak point is reached at the mid BMEP range of approximately 6 bar and at the highest engine speed of 4000rpm for this simulation.

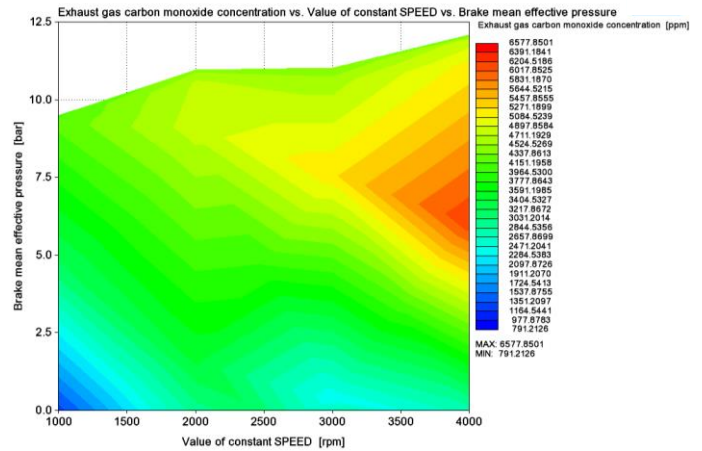


Figure 9 Part load base CO emission (ppm)

The BSFC contour plots presented in Figure 8 are part load simulated results plotted against BMEP and engine speed. Figure 8 is plotted for BMEP represented by the same throttle angles as in Figure 7; therefore the BMEP range is limited and produces a non- rectangular plotted area. However, both figures indicate that the peak BSFC is reached at the lowest throttle angle (or BMEP) and highest engine speed point which is 30 deg throttle (or approx. 1bar BMEP) at 4000rpm.

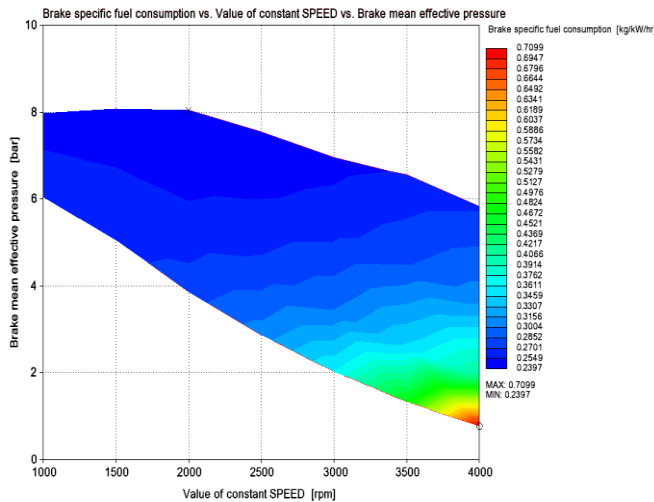


Figure 8 Part load base BSFC vs BMEP

The simulated NO<sub>x</sub> emission results of the base engine at part load are presented in Figure 10. The test was conducted for throttle angles between 30-90 deg with engine speed being varied between 1000 - 4000rpm as before. The peak NO<sub>x</sub> emission point is reached at approximately 11 bar BMEP and 2000rpm with the minimum being reached at the lowest BMEP and highest engine speed.

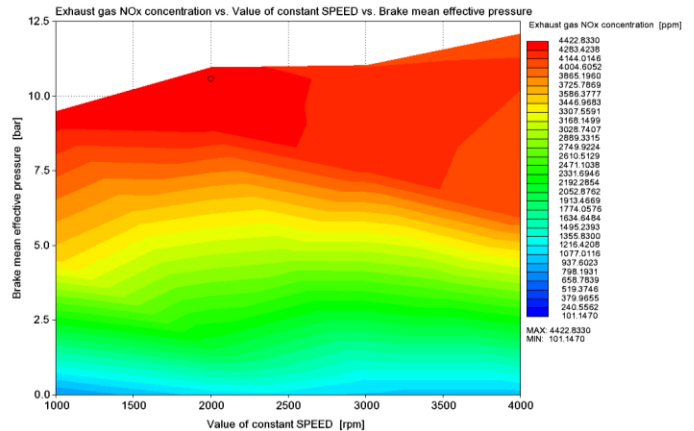


Figure 10 Part load base NOx emissions (ppm)

## Part load CDA+VVA simulation results

The part load simulations results of the CDA+VVA model are presented in this section. Part load operating points are achieved by controlling the throttle angle which in turn controls the amount of air entering the intake manifold. Therefore to maintain the defined constant air to fuel ratio, the proportional fuel injectors reduce the amount of fuel supplied. This results in part load simulated engine operation.

Figure 11 shows a time plot for engine torque pulsations against the crank angle at several throttle angle and speed combinations. The effect of the deactivated cylinders on the cyclic engine torque is evident from this plot. Furthermore, reduced engine speed at the same throttle angle is seen to produce a lower maximum torque. This is an important finding when considering NVH levels caused by CDA and identifying an optimum operating window.

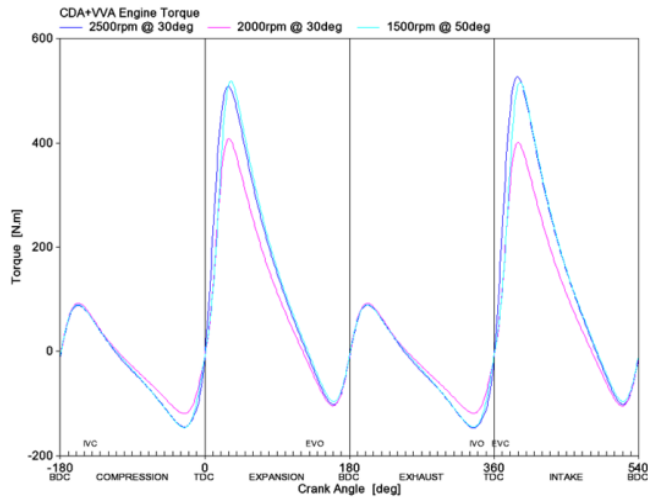


Figure 11 Part load CDA+VVA engine torque pulsations

To create the BSFC contour plots, simulations were carried out on the CDA+VVA model by setting up throttle angle sub-cases between 30 deg to 42 deg for each engine speed case and the resulting plot may be seen in Figure 12. BMEP is used as the variable in the plot to observe the behaviour of BSFC at different engine speeds. The peak BSFC point is obtained at 1.25 bar BMEP (30 deg throttle angle) and 4000rpm. The minimum BSFC range is observed at around 4.5 bar BMEP (42 deg throttle angle) between 2000 – 3000 rpm.

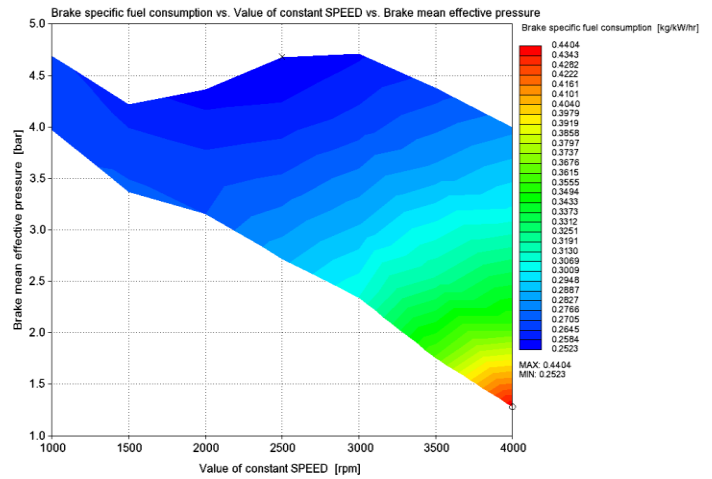


Figure 12 Part load CDA+VVA BSFC vs BMEP

The simulated CO emissions results for CDA+VVA at part load are given in Figure 13. The test was conducted for throttle angles varied between 20-90 deg with engine speed being varied between 1000 – 4000 rpm. The peak point is reached at approximately 4.5 bar and 4000 rpm. The contour distribution indicates that rising loads up to approximately 4.5 bar BMEP at constant engine speed result in increased CO emissions. The plot also indicates that low BMEP and low engine speed regions benefit from low CO emissions.

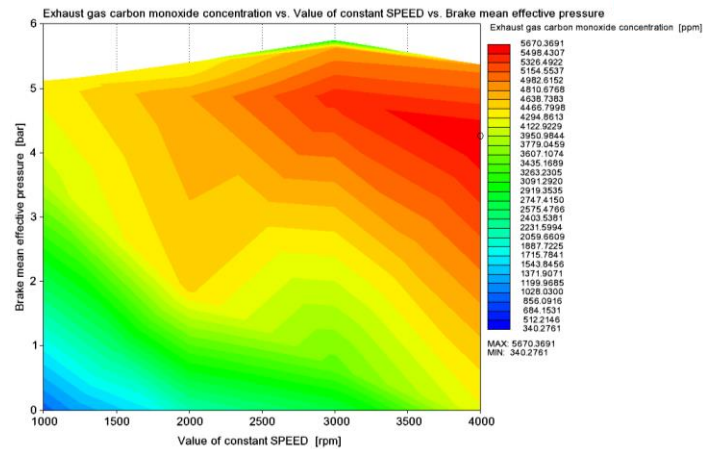


Figure 13 Part load CDA+VVA CO emission (ppm)

The simulated NO<sub>x</sub> emission results for the CDA+VVA model at part load are presented in Figure 14. The test was conducted for throttle angles between 20 - 90 deg with engine speeds being varied between 1000 – 4000 rpm. The peak NO<sub>x</sub> emission point was reached at approximately 5 bar BMEP and 1000rpm with the minimum point being reached at the lower BMEP and low engine speed region. The higher engine load region of approximately 5 bar BMEP is seen to produce high NO<sub>x</sub> emissions.

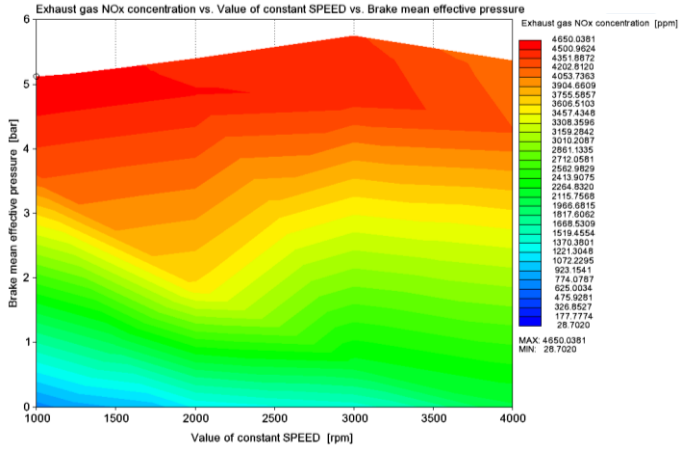


Figure 3 Part load CDA+VVA NOx emissions (ppm)

### PMEP comparison

Figures 15 and 16 show PMEP comparisons for 1000rpm and 4000rpm respectively. The PMEP results produced similar trends at 2000rpm and 3000rpm and are therefore not provided here. A significant reduction in PMEP between CDA+VVA and base cases was obtained and can be directly attributed to the pumping work savings arising due to the deactivation of two of the cylinders.

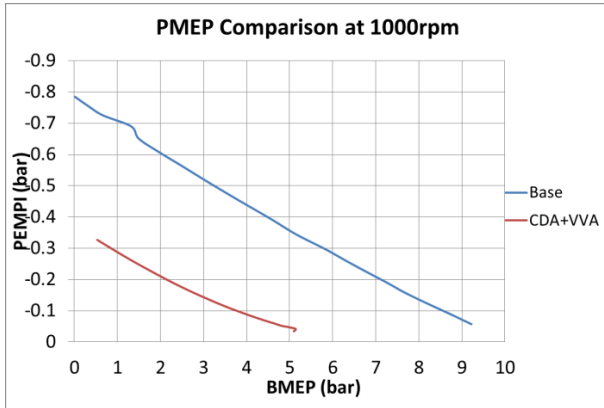


Figure 15 PMEP comparisons at 1000rpm

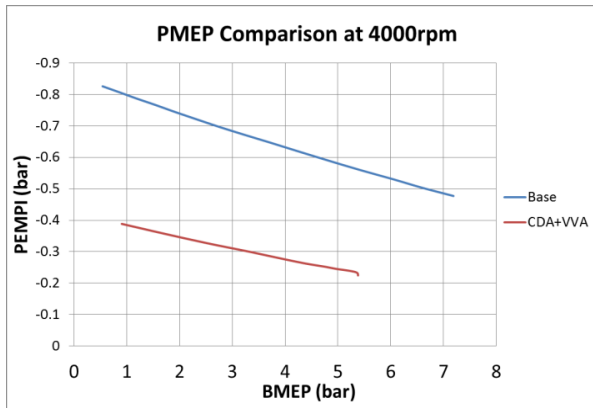


Figure 16 PMEP comparisons at 4000rpm

### BSFC benefit matrix for the CDA+VVA model

The post-processed part load results obtained from CDA+VVA and base simulations were then used to analyse the BSFC benefits at similar engine load conditions. Since BMEP was not a controllable variable in the simulations, but rather an output of the simulations, an average BMEP was calculated at each load point using the individual BMEPs of all engine speeds.

$$BSFC \text{ benefit } \% = \left( \frac{Base \text{ BSFC} - CDA \& VVA \text{ BSFC}}{Base \text{ BSFC}} \right) \% \quad (1)$$

To calculate the percentage of BSFC benefits, similar operating points on CDA+VVA and base models were first identified using BMEP and engine speed as mapping points. The corresponding BSFC values of the CDA+VVA model was deducted from and then divided by the base BSFC value as shown in Equation 1, to arrive at the actual percentage. The final BSFC result matrix is provided in Table 5 with the corresponding percentage BSFC benefits.

Table 2 BSFC benefits matrix

| Engine Speed | Average BMEP(bar) |        |        |        |       |       |
|--------------|-------------------|--------|--------|--------|-------|-------|
|              | 1.6               | 2.5    | 3.3    | 4.2    | 4.7   | 5.2   |
| 1000rpm      | 15.01%            | 9.88%  | 12.13% | 11.09% | 8.72% | 8.08% |
| 1500rpm      | 18.12%            | 13.61% | 11.28% | 10.88% | 9.97% | 7.93% |
| 2000rpm      | 13.35%            | 11.71% | 9.67%  | 9.27%  | 8.34% | 7.20% |
| 2500rpm      | 13.09%            | 9.91%  | 8.06%  | 7.52%  | 8.01% | 6.36% |
| 3000rpm      | 14.98%            | 10.22% | 8.78%  | 7.39%  | 7.29% | 6.30% |
| 3500rpm      | 13.00%            | 9.82%  | 6.25%  | 6.44%  | 7.48% | 6.97% |
| 4000rpm      | 15.07%            | 9.14%  | 8.97%  | 7.84%  | 6.68% | 7.01% |

Figure 17 shows the surface plot of the above matrix with the region in purple marking the highest percentage BSFC benefit. All observed operating points show a minimum of 5-10% BSFC percentage benefit with a maximum recorded benefit of 18.1%.

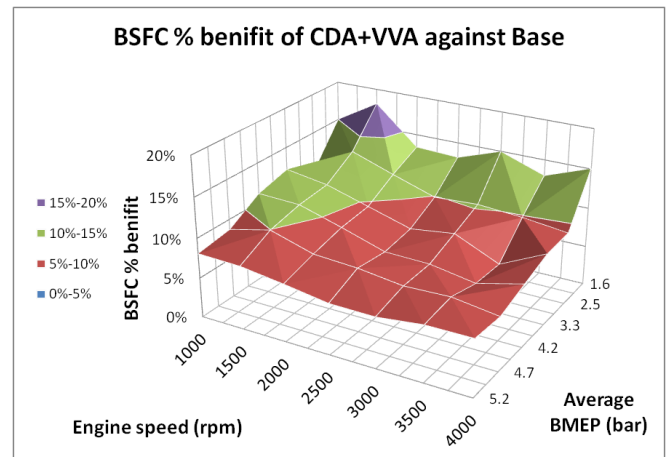


Figure 17 BSFC % benefit surface plot



## Analysis

Part load simulations performed at selected engine speeds have shown BSFC improvements with the CDA+VVA case against the base engine case. However, it is more useful to analyse the BSFC in terms of percentage improvements as shown in Table 5. The method of BSFC benefits contour mapping against engine speed and BMEP has been successfully demonstrated by [5] and [11].

Referring to Figure 18, BSFC improvements in the 15-20% band (actual highest at 18.1%) can be seen at engine speeds between 1000rpm to 1750rpm and loads below 2.5 bar average BMEP. In addition, 67% of the operating points studied offer at least 5-10% BSFC improvement for engine speeds between 1000rpm-4000rpm and below 5.2 bar average BMEP. It is also noteworthy that as the engine load increases for a given engine speed, the BSFC improvements decrease.

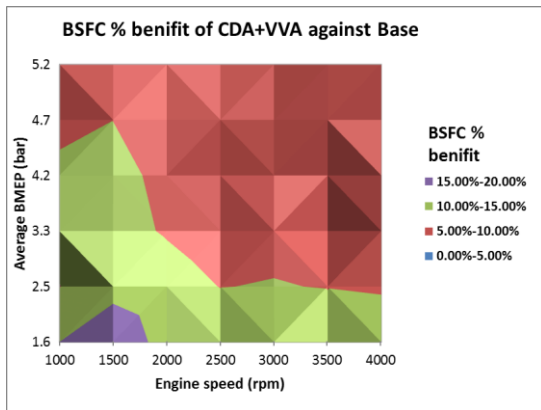


Figure 18 BSFC % benefit contour plot

These findings are in agreement with [5] who showed 8-16% BSFC improvement in similar operating conditions. However, [11] shows BSFC improvements of over 20% for engine speeds between 1000rpm-4000rpm at loads below 1bar BMEP with an engine equipped with an electro-mechanical valvetrain and valve deactivation system.

BMEP and engine speed were used as the operating condition comparison basis by which to demonstrate the possibility of performance improvements in terms of BSFC. Emissions performance however did not show clear improvements as expected but trends within the operating matrix can be identified to produce a CDA+VVA operating window. Therefore the discussion in this section will focus on identifying a suitable operating window for CDA+VVA operation with consideration to BSFC, emissions and some NVH factors which can be deduced from the presented results.

When BSFC improvement is considered on its own, the operating window encompassing 1.6 bar to 5 bar BMEP and 1000rpm to 4000rpm engine speed shows a minimum BSFC improvement of 6.25%. However, within this broad operating window, more than 60% of the region only shows 5-10% BSFC improvement and to identify a more refined operating window the emission results also need to be considered concurrently with fuel savings.

Figures 19 and 20, respectively, contain CO and NO<sub>x</sub> emissions plots, respectively, overlaid with BSFC% improvements. The area below the line depicts a minimum of 10% BSFC improvement and the area above depicts less than 10% BSFC improvements. It can be clearly seen from these plots that by operating below 2 bar BMEP and engine speeds between 1000rpm to 3500rpm, a BSFC improvement more than 10% can be achieved while maintaining CO emissions below 4000ppm and NO<sub>x</sub> emissions below 3500ppm. Rising BMEP results in increased CO and NO<sub>x</sub> emissions and only provide BSFC improvements of less than 10%.

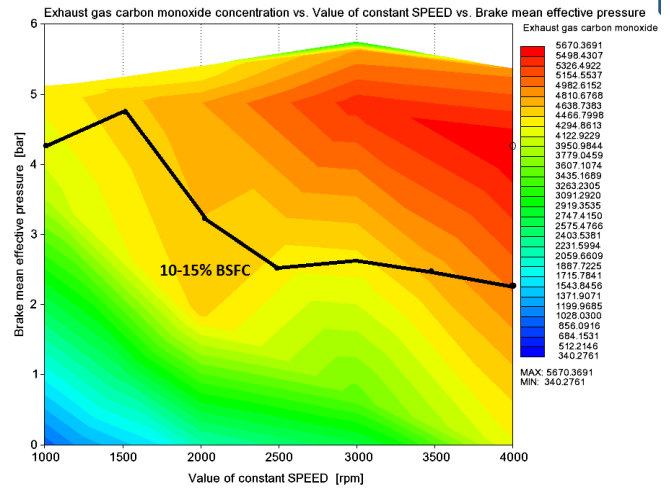


Figure 19 Part load CDA+VVA CO emissions with BSFC overlay

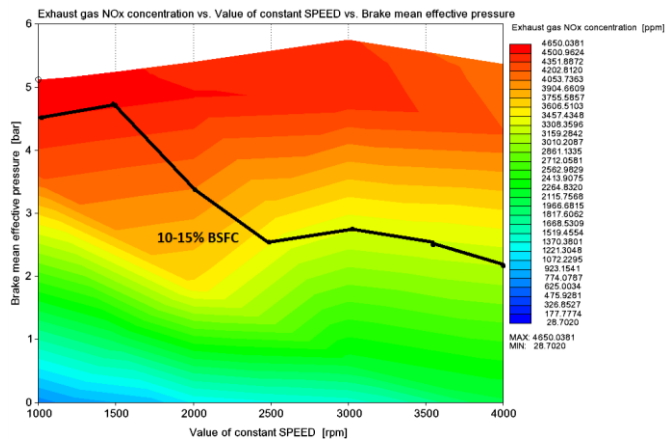


Figure 20 Part load CDA+VVA NOx emissions with BSFC overlay

Another factor affecting the optimal CDA operating window is NVH. Even though this study does not contain a dedicated section for NVH analysis, the results presented for engine torque over the operating cycle for CDA+VVA indicate that at constant load (constant throttle angle) a rise in engine speed leads to higher amplitudes of pulsation. Higher amplitude torque pulsations lead to increased NVH and act as a constraint to the CDA operating window [6]. Therefore an operating window with low engine speed is preferable. Active engine mounts [7] and damping torque converters have been adopted as possible solutions to minimise this adverse NVH effect.

After considering BSFC, emissions and elements of NVH, it may be argued that the most optimal operating window for the CDA+VVA engine discussed in this study would be between 1 bar to 2 bar BMEP and 1000rpm to 3500rpm engine speed. Studies by [5], [8] and [11] confirm similar operating windows with [11] pointing out the inclusion of the NEDC (New European Driving Cycle) operating points within this selected CDA operating window thereby affirming to an extent the usefulness of CDA and VVA in this region.

## Conclusions

The study presented in this paper is a contribution to the on-going discussion of integrating CDA and VVA technologies to improve part load gasoline engine performance. The main motivators for performance improvements in gasoline engines are increasingly stringent regulations demanding further reductions in engine emissions. Part load engine operation is significantly less efficient than WOT gasoline engine operation which leads to increased fuel consumption and emissions. Therefore, the final benefit would be fuel cost saving for the end users of vehicles equipped with such engines as well as reduced emissions to the environment.

The data analysed provide results which support the argument that integrating CDA and VVA can improve part load engine BSFC as discussed. A reduction in BSFC inevitably means a reduction in CO<sub>2</sub> emission which is a major outcome of this study. CO and NO<sub>x</sub> emissions however have not yielded considerable improvements and in certain cases showed a negative impact. A dedicated study in this area would be required.

It was identified that CDA+VVA operation for loads between 1 bar to 2bar and engine speeds between 1000rpm to 3500rpm offers a BSFC improvement of 10-20% at moderate CO and NO<sub>x</sub> emissions. The implication of NVH in CDA applications is also discussed briefly along with its importance as a key factor for identifying optimal operational window. Rising engine speeds and increasing torque pulsation amplitudes lead to higher NVH. Therefore, engine speeds below 4000rpm are recommended for CDA operation.

The decision to integrate CDA and VVA into a gasoline engine cannot however be made purely on a basis of performance benefit. Cost, complexity and reliability of these technologies are key factors affecting a potential decision. In conclusion, CDA & VVA integration has shown significant fuel consumption and CO<sub>2</sub> emission reduction benefit for gasoline engine operation at selected part load conditions. The integration of CDA+VVA with the gasoline engine shows great potential in the active quest for efficient and environmentally friendly energy conversion technologies.

## References

1. Mock, P. "European Vehicle Market Statistics, 2012". [http://www.theicct.org/sites/default/files/publication/sPocketbook\\_2012\\_opt.pdf](http://www.theicct.org/sites/default/files/publication/sPocketbook_2012_opt.pdf), 2012 [Accessed 1 August 2013].

2. Gis, W. and Bielaczyc P., "Emission of CO<sub>2</sub> and Fuel Consumption for Automotive Vehicles." SAE International. Michigan, 1999, DOI: [10.4271/1999-01-1074](https://doi.org/10.4271/1999-01-1074).
3. KPGM. "KPMG's Global Automotive Executive Survey 2013 (Global version)". <http://www.kpmg.com/Global/en/IssuesAndInsights/ArticlesPublications/global-automotive-executive-survey/Documents/2013-report-v4.pdf>, 2013 [Accessed 1 Aug. 2013].
4. Fontana, G., Galloni E., and Torella E., "Experimental and Numerical Analysis of a Small VVT S.I. Engine." SAE Naples, Italy, 2005, DOI: [10.4271/2005-24-079](https://doi.org/10.4271/2005-24-079).
5. Flierl, R., Lauer F., Breuer M., and Hannibal W., "Cylinder Deactivation with Mechanically Fully Variable Train." SAE Int. J. Engines, 5(2) : 207-25, 2012.
6. Leone, T., and M. Pozar., "Fuel Economy Benefit of Cylinder Deactivation - Sensitivity to Vehicle Application and Operating Constraints." SAE International. Michigan, 2001, DOI: [10.4271/2001-01-3591](https://doi.org/10.4271/2001-01-3591).
7. Birch, S., "VW debuts cylinder deactivation on 2012 V8 and I4 engines." <http://www.sae.org/mags/aei/10189>, 2012 [Accessed 1 Aug 2013].
8. Falkowski, A., McElwee M., and Bonne M., "Design and Development of the DaimlerChrysler 5.7L HEMI® Engine Multi-Displacement Cylinder Deactivation System." SAE International. Michigan, 2004, DOI: [10.4271/2004-01-2106](https://doi.org/10.4271/2004-01-2106).
9. Paimon, A. S. B., Rajoo S., and Jazair W., "Engine induction strategy for part load operation towards low carbon vehicle." Project Proposal, Malaysia: MJIT, Universiti Teknologi Malaysia, 2013.
10. Boretti, A., and Scalco J., "Piston and Valve Deactivation for Improved Part Load Performances of Internal Combustion Engines", SAE International. Michigan, 2011, DOI: [10.4271/2011-01-0368](https://doi.org/10.4271/2011-01-0368).
11. Kreuter, P., Heuser P., Reinicke-Murmann J., Erz R., Stein P., and Peter U., "Meta - CVD System An Electro-Mechanical Cylinder and Valve Deactivation System." SAE International, Michigan, 2001, DOI: [10.4271/2001-01-0240](https://doi.org/10.4271/2001-01-0240).

## Acknowledgments

The authors would like to thank Proton Holdings Bhd. (Malaysia) for permission to use the engine data. Special thanks also go Malaysian Ministry of Higher Education for funding vot 4L083 in the current project.

## Definitions/Abbreviations

|                       |   |
|-----------------------|---|
| <b>BMEP</b>           | Brake Mean Effective Pressure                         |
| <b>BSFC</b>           | Brake specific fuel consumption                       |
| <b>CDA</b>            | Cylinder Deactivation                                 |
| <b>CO</b>             | Carbon Monoxide                                       |
| <b>CO<sub>2</sub></b> | Carbon Dioxide  |
| <b>Deg</b>            | degrees (angle)                                       |
| <b>DOE</b>            | Design of Experiments                                 |
| <b>EVDUR</b>          | Exhaust valve duration                                |
| <b>EVML</b>           | Exhaust valve maximum lift                            |
| <b>EVMP</b>           | Exhaust valve maximum lift point                      |
| <b>GHG</b>            | Greenhouse gas  |
| <b>IC</b>             | Internal combustion                                   |
| <b>IMEP</b>           | Indicated mean effective pressure                     |
| <b>IVDUR</b>          | Inlet valve duration                                  |
| <b>IVML</b>           | Inlet valve maximum lift                              |
| <b>IVMP</b>           | Inlet valve maximum lift point                        |
| <b>MJITT</b>          | Malayasia-Japan International Institute of Technology |
| <b>NEDC</b>           | New European Driving Cycle                            |
| <b>NVH</b>            | Noise Vibration and Harshness                         |
| <b>NOx</b>            | Nitrogen Oxide  |
| <b>PMEP</b>           | Pump Mean Effective Pressure                          |
| <b>RPM</b>            | Revolutions per minute                                |
| <b>SI</b>             | Spark Ignition  |
| <b>UTM</b>            | Universiti Teknologi Malaysia                         |
| <b>VVA</b>            | Variable Valve Actuation                              |